

## Unoccupied band structure of the Nb(110) surface

P. D. Johnson and Xiaohe Pan

*Physics Department, Brookhaven National Laboratory, Upton, New York 11973*

(Received 6 April 1988)

Inverse-photoemission spectra (IPES) recorded from Nb(110) allow the unoccupied bands to be mapped. The critical points are identified and the approximate form of the high-lying  $\Sigma_1$  band established. This latter band serves as the initial state in IPES and the final state in photoemission studies. It is suggested that disagreement between theory and experiment for the  $T_{25'}$  critical point probably reflects the presence of a surface resonance. Fluorescence is also observed from the decay of the Nb  $4p$  core holes. The relative intensity of the fluorescence due to  $4p_{3/2}$  and  $4p_{1/2}$  core holes is discussed in terms of possible Coster-Kronig transitions.

### I. INTRODUCTION

Over the past two decades the band structure of niobium has been the subject of several first-principles calculations.<sup>1-4</sup> However, this theoretical effort has not been matched by an equivalent number of experimental band-structure studies.<sup>5,6</sup> Indeed, photoemission studies, which have examined the electronic structure of clean Nb(110) rather than its adsorption properties, highlighted a key problem. In any band-mapping exercise derived from photoemission data, it is important that, for direct transitions between two bands, some suitable form be chosen for the high-lying final-state band. In a number of studies on other metals this band has either been obtained from first-principles calculations where these exist or approximated by a free-electron-like band.<sup>7</sup> For niobium the calculations have tended not to consider the higher bands and a free-electron-like final state does not appear to represent a good approximation. The latter limitation arises from the fact that the final-state  $\Sigma_1$  band results from strong hybridization between the  $sp$  band and the unoccupied  $d$  bands. An earlier photoemission study of the Nb(110) surface examined the validity of a rigid band-shift approximation.<sup>5</sup> Thus the final-state band was approximated by shifting the equivalent band calculated for neighboring molybdenum.<sup>8</sup> With this approach the authors were able to draw several conclusions about the band structure of niobium.

In this paper we present an inverse-photoemission study of the unoccupied bands of the clean Nb(110) surface. Our study allows us to identify the unoccupied critical points at the  $\Gamma$  point and to make an improved approximation of the higher-lying  $\Sigma_1$  band. For inverse-photoemission studies this band serves as the initial state. Using this approximation we are able to map the unoccupied bands above the Fermi level and compare these with calculations. We find reasonable agreement between recent calculations and experiments for the  $\Gamma_{12}$  point but not for the  $\Gamma_{25'}$  point. In Sec. II of this paper we describe our experimental arrangement, and present our results. We also show spectra which include fluorescence peaks resulting from the decay of the  $4p_{3/2}$  core hole. There is no obvious fluorescence from the  $4p_{1/2}$  core hole and it is

suggested that this may reflect Coster-Kronig transitions. In Sec. III we discuss these data and present our conclusions.

### II. EXPERIMENT

The inverse-photoemission studies described in this paper were carried out using a grating spectrograph that has been described in detail elsewhere.<sup>9</sup> Using such an apparatus it is possible to determine the unoccupied band structure as a function of  $k_{\perp}$  at a fixed  $k_{\parallel}$  from inverse-photoemission spectra recorded at different incident-electron energies. We demonstrate this in Sec. III.

The niobium (110) surface used in these studies was obtained by resistively heating a niobium foil to approximately 2300°C. As in a number of previous studies,<sup>10</sup> low-energy electron diffraction (LEED) indicated that following this treatment the foil recrystallized with the  $\langle 110 \rangle$  direction along the surface normal. Surface cleanliness was monitored using Auger-electron spectroscopy.

In Fig. 1 we show the inverse photoemission spectra recorded from the Nb(110) surface as a function of the incident-electron beam energy. It will be seen in the figure that as the electron-beam energy is reduced from approximately 20 to 13 eV, one band disperses from an energy 1.5 eV above the Fermi level down to the Fermi level and then back again to approximately the same binding energy. A second band further from the Fermi level at an energy of approximately 3.5 eV splits into two bands as the incident-electron beam energy is reduced.

By applying optical selection rules<sup>11</sup> we are able to label the symmetry of these bands. The initial state band in inverse photoemission is required to be a totally symmetric  $\Sigma_1$  band. With this limitation the allowed final-state bands will fall into  $\Sigma_1$ ,  $\Sigma_3$ , and  $\Sigma_4$  representations. We thus identify the band dispersing down to the Fermi level and back with the  $\Sigma_1$  band predicted in all calculations.<sup>1-4</sup> We associate the other bands with the  $\Sigma_4$  and  $\Sigma_1$  bands dispersing away from the  $\Gamma_{12}$  point. We do not appear to observe the  $\Sigma_3$  band which is calculated to disperse away from the  $\Gamma_{25'}$  point.

In Fig. 2 we again show inverse-photoemission spectra for electrons incident along the surface normal but now

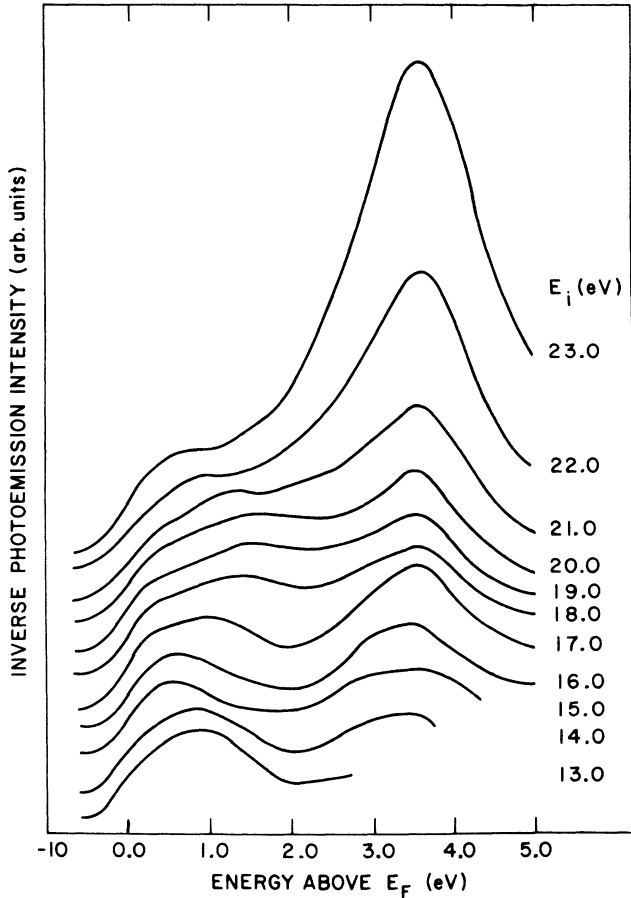


FIG. 1. Inverse-photoemission spectra recorded from Nb(110) as a function of the incident electron-beam energy  $E_i$  determined with respect to the Fermi energy. The electron beam is incident along the surface normal.

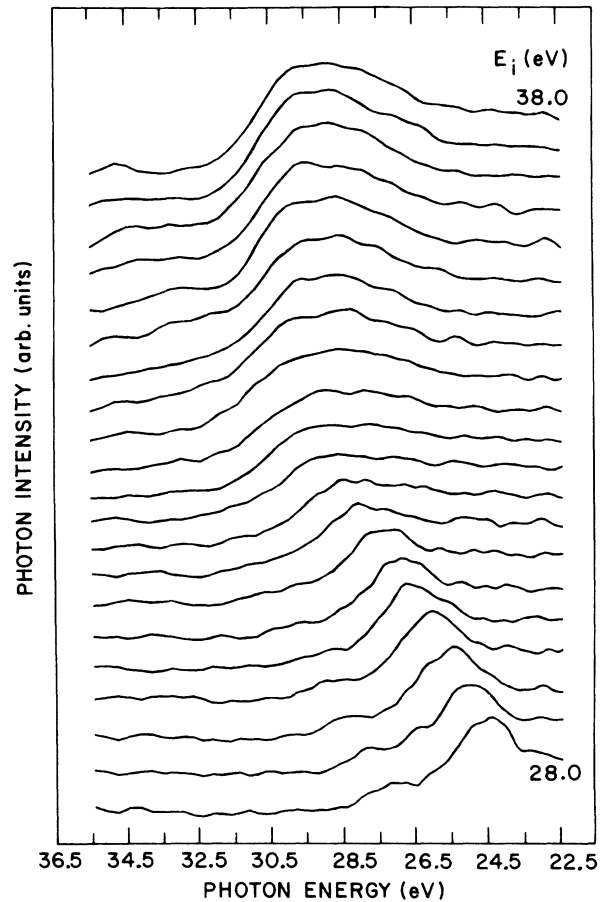


FIG. 2. Inverse-photoemission spectra recorded as in Fig. 1 but over a higher energy range. The incident-electron beam energy  $E_i$  ranges in 0.5-eV steps from 28 to 38 eV with respect to  $E_F$ .

with energies spanning a higher energy range. This series of spectra reveals another feature. Above 31 eV, the threshold for excitation of the  $4p_{3/2}$  core hole, we begin to observe photons emitted at a constant photon energy characteristic of the radiative decay of these holes. This fluorescence or soft-x-ray emission is not a new phenomenon and is to be expected to an inverse-photoemission apparatus of this type. Indeed a fluorescent peak at constant photon energy is the direct analogue of an Auger peak at constant electron energy in a photoemission spectrum. Examination of Fig. 2 reveals little or no fluorescence characteristic of the radiative decay of the  $4p_{1/2}$  core hole.

### III. DISCUSSION

We firstly discuss the radiative decay of the  $4p$  core holes. In order to get a quantitative feel for the relative intensity that might be expected from decay of the  $4p_{3/2}$  and  $4p_{1/2}$  core holes we follow the analysis of soft x-ray emission due to Mattheiss and Dietz.<sup>12</sup>

They show that if the emission intensity  $I_{nlj}$  of photons emitted from the radiative decay of a core state  $\langle I_{nlj} \rangle$  is given by

$$I_{nlj} = n_{nlj} k_{nlj}^r, \quad (1)$$

where  $n_{nlj}$  and  $k_{nlj}^r$  are the number of excited states and radiative-decay rate, respectively, then the ratio of the intensities for the two spin-orbit-split core levels will be given by

$$\frac{I_{nlj}}{I_{nlj'}} = \frac{(2j+1)k_{nlj}^r}{(2j'+1)k_{nlj'}^r}. \quad (2)$$

Using the tables and formulas given by Mattheiss and Dietz and further, assuming spin orbit effects are small in the valence band of niobium, we find that the intensity ratio of the radiative decay of the two core levels,  $4p_{3/2}$  and  $4p_{1/2}$ , will be by approximately 4.0. The assumption of an intensity ratio simply reflecting the multiplicity of the core levels with complete neglect of selection rules would lead to a ratio of 2.0. The intensity ratio in Fig. 2 is clearly much higher than 4.0. Indeed we note that a similar imbalance in the intensity ratio has been observed in soft x-ray emission from the outer core levels of the free-electron metals.<sup>13</sup> One assumption made in the analysis outlined above is that  $k^{nr}$ , the nonradiative decay rate, is approximately the same for both core levels. This

is probably valid for Auger decay but neglects the possibility of decay via fast Coster-Kronig transitions for the  $4p_{1/2}$  core level. It is anticipated that inclusion of this decay channel will lead to a much higher value for the intensity ratio.

Finally we note that above threshold for excitation of the  $4p$  core holes the intensity of the direct transitions of the inverse-photoemission process show a marked reduction indicating competition between the two channels.

We now turn to a discussion of the experimentally observed band dispersions shown in Fig. 1. In order to map out the dispersion of the final-state bands with  $k_{\parallel}$  some knowledge of the dispersion of the initial-state band is required. As noted earlier, one approach to this problem would be to use a free-electron-like dispersion for the high-lying initial state. This approximation does not allow for any band gaps introduced by the periodic potential but has proved very useful in a number of earlier photoemission studies. To apply this to the present experiments, one simply adopts a free-electron dispersion determined from  $k_{\parallel}^2$  and measured from some inner potential; the latter being set equal to the calculated value or adjusted to fit the experimental data. If the inner potential is taken from calculation<sup>1</sup> this procedure locates the  $\Gamma$  critical point of the initial-state band in the TN direction at approximately 23 eV above the Fermi level. Examination of the experimental data in Fig. 1. shows that the  $\Sigma_1$  final-state band reverses its dispersion at incident-electron energies around 20 eV with respect to the Fermi level. We therefore associate this region with  $\Gamma$  and consequently locate the binding energy of the initial state  $\Sigma_1$  band for this critical point at 20 eV above the Fermi level. To apply this to the present experiments, one simply adopts a free-electron dispersion determined from  $k_{\parallel}^2$  and measured from some inner potential, the latter being set equal to the calculated value or adjusted to fit the experimental data. If the inner potential is taken from calculation<sup>1</sup> this procedure locates the  $\Gamma$  critical point of the initial-state band in the TN direction at approximately 23 eV above the Fermi level. Examination of the experimental data in Fig. 1 shows that the  $\Sigma_1$  final-state band reverses its dispersion at incident-electron energies around 20 eV with respect to the Fermi level. We therefore associate this region with  $\Gamma$  and consequently locate the binding energy of the initial state  $\Sigma_1$  band for this critical point at 20 eV above the Fermi level.

To pin the initial-state band at the lower critical point we note that a recent calculation located the  $N_1$  point at 12.0 eV above the Fermi level.<sup>4</sup> Smith *et al.*,<sup>5</sup> inferred from their photoemission data that this point was located at approximately 13.0 eV above the Fermi level. As we show later the choice of 12.0 eV for this  $N_1$  point produces close agreement between our experimentally measured dispersion for the  $\Sigma_1$  band closest to the Fermi level and the calculation of Elyashar and Koelling.<sup>2</sup> Finally to obtain some approximation for the dispersion of the initial-state band we follow the earlier photoemission study and adopt the shape of the equivalent band calculated for neighboring molybdenum. Thus we take the calculated  $\Sigma_1$  band from the Mo calculation of Zunger *et al.*<sup>8</sup> and scale it to pass through the higher critical

point determined experimentally and the  $N_1$  point 12 eV above the Fermi level.

In Fig. 3 we plot the dispersion of the experimental final-state points determined by the above procedure. These experimental observations are indicated by vertical bars, the length of which may be taken as a measure of the error in determining the energies. In the figure we also compare our empirically determined initial-state band with the free-electron-like band. We have included the results of a first principles calculation of the "final-state" bands due to Elyashar and Koelling.<sup>2</sup>

It will be seen that the overall comparison is good with excellent agreement for the  $\Gamma_{12}$  critical point and the dispersion of the  $\Sigma_4$  and upper  $\Sigma_1$  band. The general shape of the experimental lower  $\Sigma_1$  band is in reasonable agreement with the calculation, there being an indication

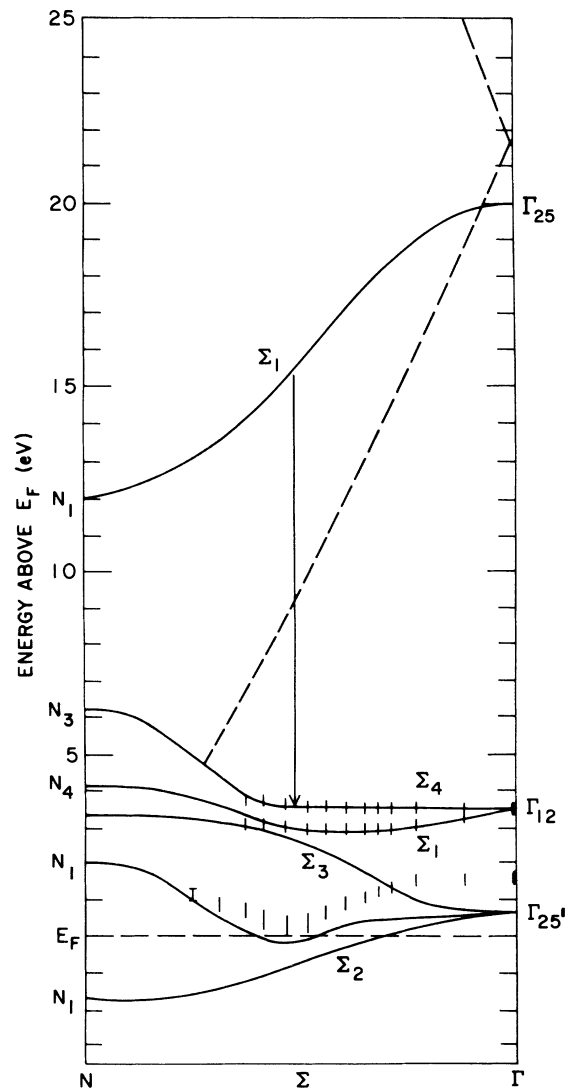


FIG. 3. Dispersion of the unoccupied bands above the Fermi level for the Nb(110)  $\Sigma$  direction as determined from the data in Fig. 1. The experimental observations are indicated by the vertical dashed lines. The solid lines are from the theoretical calculation of Ref. 2. The high-lying  $\Sigma_1$  band used for plotting this dispersion is compared with a free-electron band (dashed line).

that the band disperses down below the Fermi level before dispersing upwards again. Indeed this supports the assignment of a peak close to the Fermi energy in the earlier photoemission studies<sup>5</sup> to the same  $\Sigma_1$  band. The peak was observed in photoemission spectra for photon energies around 15 eV, which corresponds to the incident electron energies (defined with respect to the Fermi level) at which the  $\Sigma_1$  band appears to be close to or below the Fermi level in the present experiment.

The most obvious disagreement between theory and experiment occurs at the  $\Gamma_{25'}$  critical point. This disagreement is particularly surprising in view of the good agreement for the  $\Gamma_{12'}$  point. In Table I we compare our experimentally determined values of these  $\Gamma$  critical points with a number of different calculations. It will be seen that in general good agreement is found between the experiment and modern self-consistent calculations for the  $\Gamma_{12}$  point but all calculations place the  $\Gamma_{25'}$  point closer to the Fermi level. Of course any agreement may be purely fortuitous in that we are comparing an experimentally determined excited state with a calculation of the ground state. Indeed the difference between the experimentally observed energies and the density-functional calculation of the band structure reflects the real component of the self-energy of the final electron state. However model calculations suggest that within 5 eV of the Fermi level this difference should be small.<sup>14,15</sup>

Possible explanations for the discrepancy between our experiment and the theoretical positioning of the  $\Gamma_{25'}$  point include misalignment of the sample, the presence of the boundaries of the large crystallites, or the presence of electronic surface states and resonances. We believe that any misalignment of the sample was minimal. Indeed, spectra recorded away from the surface normal indicated that the high  $\Sigma_1$  and  $\Sigma_4$  bands had their minimum separation at the surface normal. Finally, without experiments on a full single crystal it is not possible to assess the influence of the crystallite sizes in the recrystallized foil. However, we note that an earlier angle-resolved photoemission study<sup>16</sup> of a palladium monolayer grown on a similar niobium substrate did not appear to be influenced by crystallite size. Unoccupied resonances situated near the center of the surface zone and at an appropriate ener-

TABLE I. Comparison of the critical points determined in different calculations with the experimentally observed points. The references of the different calculations are indicated.

| Reference | $\Gamma_{25'}$ | $\Gamma_{12}$ | $\Gamma_{12} - \Gamma_{25'}$ |
|-----------|----------------|---------------|------------------------------|
| 1         | 0.34           | 2.6           | 2.26                         |
| 2         | 0.52           | 3.45          | 2.93                         |
| 3         | 0.19           | 3.18          | 2.99                         |
| 4         | 0.43           | 2.72          | 2.29                         |
| Expt.     | 1.6            | 3.5           | 1.9                          |

gy above the Fermi level have been predicted in a recent slab calculation of the niobium (110) surface.<sup>17</sup> Thus the possibility exists of a transfer of oscillator strength from the bulk band to a close-lying resonance for values of  $k_{\perp}$  corresponding to the center of the zone. Indeed such a transfer of intensity between bulk bands and surface states has previously been observed in an inverse-photoemission study.<sup>18</sup>

In summary, we have used inverse photoemission to map out the unoccupied  $d$  bands of niobium. We have found reasonable agreement between the experimentally determined dispersion and theoretical calculations. Our study has allowed us to determine the form of the initial  $\Sigma_1$  band. We find that this band is well removed in shape from a free-electron-like band due to strong hybridization effects. We have also determined the critical points at the center of the zone. The agreement is particularly good for the  $\Gamma_{12}$  point but a discrepancy exists in the measured  $\Gamma_{25'}$  point. We suggest that this discrepancy is possibly due to the presence of surface resonances at the center of the zone.

Our measurements of the fluorescent decay of the  $4p$  core levels show that this emission is dominated by radiative transitions into the  $4p_{3/2}$  core level. We suggest that Coster-Kronig decay of the  $4p_{1/2}$  level may lead to this imbalance.

#### ACKNOWLEDGMENT

This work was supported by the Division of Materials Sciences, U.S. Department of Energy, under Contract No. DE-AC02-76CH00016.

<sup>1</sup>L. F. Mattheiss, Phys. Rev. B **1**, 373 (1970).

<sup>2</sup>N. Elyashar and D. Koelling, Phys. Rev. B **15**, 3620 (1977).

<sup>3</sup>C. L. Fu and K. M. Ho, Phys. Rev. B **28**, 5480 (1983).

<sup>4</sup>J. D. Shore and D. A. Papaconstantopoulos, Phys. Rev. B **35**, 1122 (1987).

<sup>5</sup>R. J. Smith, G. P. Williams, J. Colbert, M. Sangurton, and G. J. Lapeyre, Phys. Rev. B **22**, 1584 (1980).

<sup>6</sup>R. J. Smith, Solid State Commun. **37**, 725 (1981).

<sup>7</sup>F. J. Himpsel, Adv. Phys. **32**, 1 (1983).

<sup>8</sup>A. Zunger, G. P. Kerker, and M. L. Cohen, Phys. Rev. B **20**, 581 (1979).

<sup>9</sup>P. D. Johnson, S. L. Hulbert, R. F. Garrett, and M. R. Howells, Rev. Sci. Instrum. **57**, 1324 (1986).

<sup>10</sup>M. Strongin, M. El-Batanouny, and M. Pick, Phys. Rev. B **22**, 3126 (1980).

<sup>11</sup>W. Eberhardt and F. J. Himpsel, Phys. Rev. B **21**, 5572 (1980).

<sup>12</sup>L. Mattheiss and E. Dietz, Phys. Rev. B **22**, 1663 (1980).

<sup>13</sup>P. N. First, R. L. Fink, and C. P. Flynn, J. Phys. F **17**, L29 (1987).

<sup>14</sup>P. O. Nilsson and C. G. Larsson, Phys. Rev. B **27**, 6143 (1983).

<sup>15</sup>W. Speier, R. Zelker, and J. C. Fuggle, Phys. Rev. B **32**, 3597 (1985).

<sup>16</sup>M. El-Batanouny, D. R. Hamann, S. R. Chubb, and J. W. Davenport, Phys. Rev. B **27**, 2575 (1983).

<sup>17</sup>X. Pan, P. D. Johnson, M. Weinert, R. E. Watson, G. Fernando, J. W. Davenport, and S. L. Hulbert, Phys. Rev. B (to be published).

<sup>18</sup>S. L. Hulbert, R. G. Garrett, and P. D. Johnson, Phys. Rev. B **33**, 7326 (1986).